DOE/NV/25946--012
DOE/NV/11718--1253

Optomechanical considerations for the VISAR diagnostic at the National Ignition Facility (NIF)

Morris I. Kaufman*[a] John R. Celeste[b], Brent C. Frogget[a], Tony L. Lee[b],
Brian J. MacGowan[b], Robert M. Malone[a], Edmund W. Ng[b], Tom W. Tunnell[a], Phillip W. Watts[c]
[a]NSTec, Los Alamos Operations, 182 East Gate Drive, Los Alamos, NM USA 87544;
[b]Lawrence Livermore National Laboratory, P. O. Box 808, Livermore, CA USA 94551;
[c]NSTec, Livermore Operations, 161 S. Vasco Road, Livermore, CA USA 94551

ABSTRACT

The National Ignition Facility (NIF) requires optical diagnostics for measuring shock velocities in shock physics experiments. The velocity interferometer for any reflector measures shock velocities at a location remote to the NIF target chamber. Our team designed two systems, one for a polar port orientation, and the other to accommodate two equatorial ports. The polar-oriented design requires a 48-m optical relay to move the light from inside the target chamber to a separately housed measurement and laser illumination station. The currently operational equatorial design requires a much shorter relay of 21 m. Both designs posed significant optomechanical challenges due to the long optical path length, large quantity of optical elements, and stringent NIF requirements. System design had to tightly control the use of lubricants and materials, especially those inside the vacuum chamber; tolerate earthquakes and radiation; and consider numerous other tolerance, alignment, and steering adjustment issues. To ensure compliance with NIF performance requirements, we conducted a finite element analysis.

Keywords: VISAR, optical relay, National Ignition Facility (NIF), optomechanical tolerance analysis, earthquake restraints, FEA, tolerance, gimbal, alignment

1. INTRODUCTION

The velocity interferometer for any reflector[1,2,3] (VISAR) measures the velocity of a moving surface by recording its Doppler wavelength shift. The National Ignition Facility (NIF) VISAR diagnostic is a primary means for timing the shocks induced into an ignition capsule.[4] Shocks, initiated by drive laser beams that enter into the spherical NIF target chamber through its largest ports, are focused onto a sample target. Figure 1 shows the equatorial 90-45 port location of an imaging VISAR system fielded to collect images inside a 10-m-diameter vacuum target chamber at NIF. The optical system relays the image out of the vacuum chamber and into an interferometer enclosure, where the light is split and recorded by three streak cameras.

The VISAR system will be fielded in the equatorial 90-315 port (Figure 2). Our team also designed a VISAR system for future installation at the

*kaufmami@nv.doe.gov; phone 505 663-2034; fax 505 663-2105

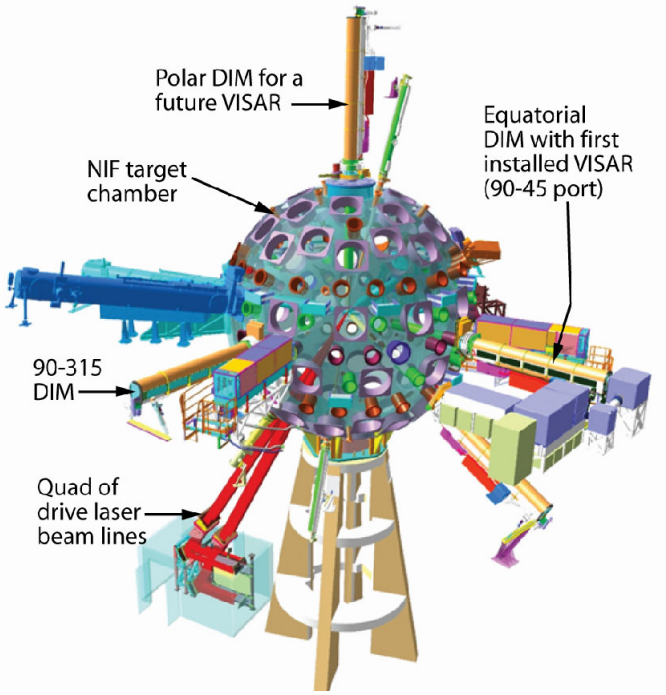

Figure 1. VISAR using the 90-45 port of the NIF target chamber (note the drive lasers)

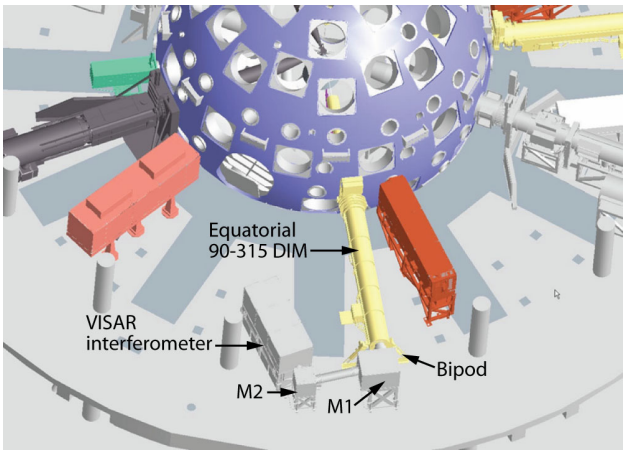

Figure 2. Mechanical layout of equatorial (90-315) VISAR

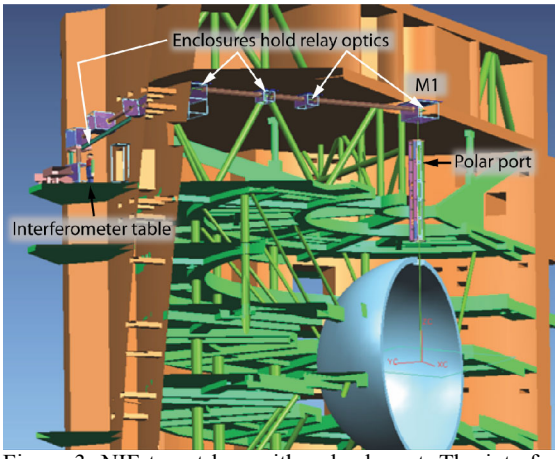

Figure 3. NIF target bay with polar layout. The interferometer (outside the containment wall) is a future installation.

0-0 (polar) target chamber port (Figure 3). In previous papers, we have discussed this project's optical and optomechanical parts.[5,6,7,8]

The VISAR interferometer enclosure houses an optical table that supports two VISAR interferometers, a thermal imaging diagnostic[8] and associated optics, and streak cameras, plus the laser launch and alignment optics. Between the vacuum chamber and the interferometer table is a series of relay lenses and mirrors that navigates the light through the densely populated NIF target bay. Inside the vacuum chamber (and 50 cm from target chamber center) is the first optical assembly, L1 (Figure 4). The NIF target bay has a roughly cylindrical shape with a diameter of 30 m (100 ft).

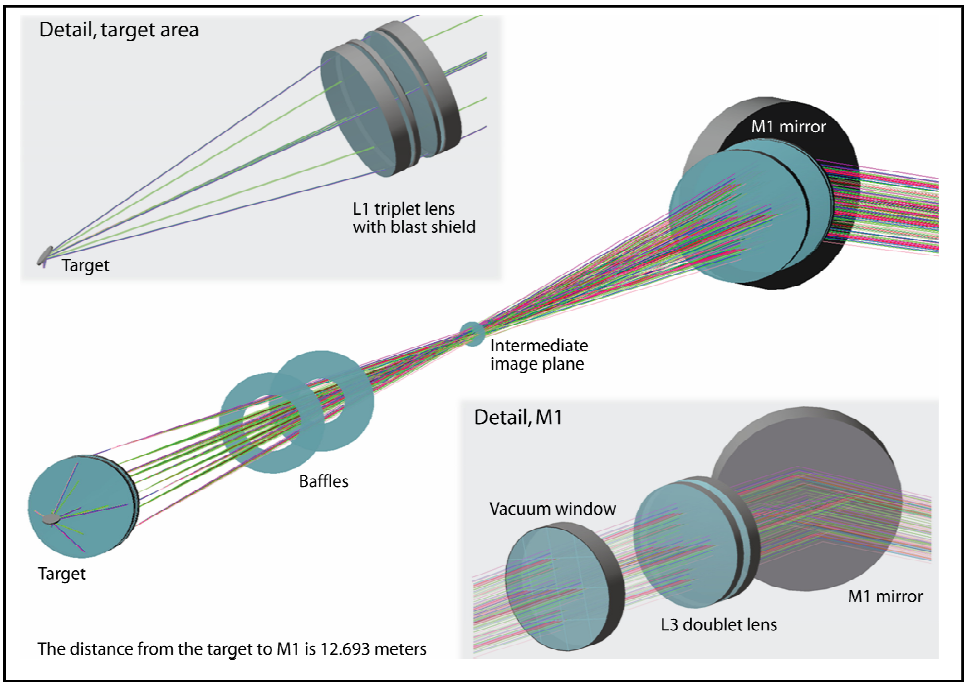

Figure 4. Optical elements near the target chamber center

Diagnostic instruments that must be inserted into the target chamber are loaded into a handling device called the diagnostic instrument manipulator (DIM). The DIM features bipod feet (Figure 2) that have a steering function.

The focusing optics inside the NIF chamber are located in a 4-m instrument cart called the DIM cart. This cart is divided into two sections and loaded into the DIM in a manner similar to loading a torpedo (Figure 5). Optical elements inside the DIM cart include a removable blast window, the first fused silica triplet lens (L1), and baffles to block background light.

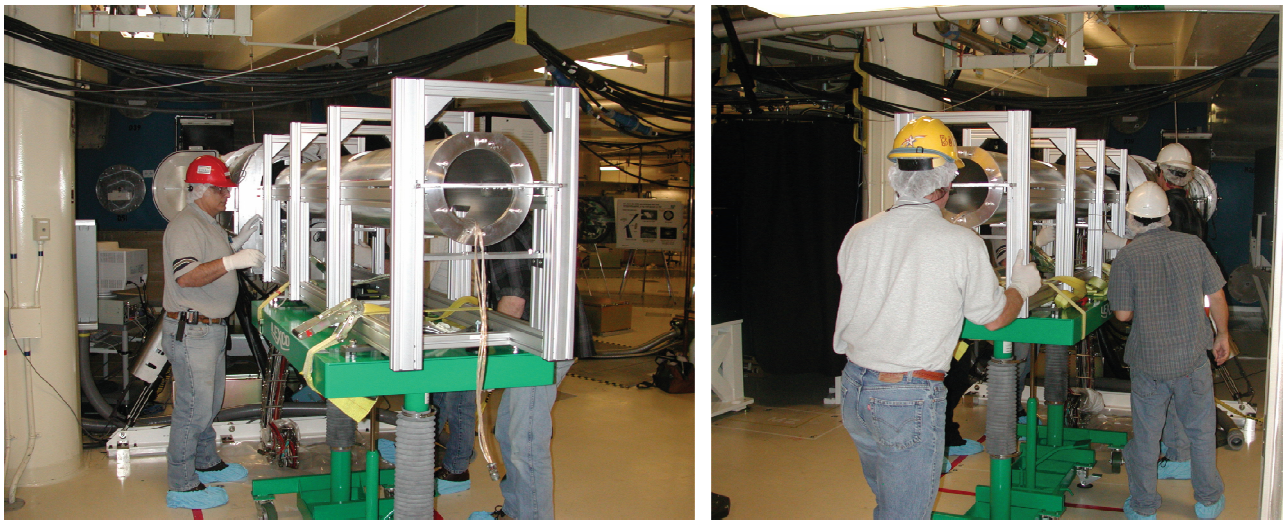
Figure 5. Two views of the insertion of the VISAR DIM cart into the DIM

2. MECHANICAL DESIGN ISSUES

NIF VISAR requirements include a 50-μm target-pointing accuracy, diffraction-limited image quality, 4-hour alignment stability, quick blast shield replacement, compliance with seismic requirements, 8-hour setup time, and compatibility with hazardous environments (sometimes both high vacuum and high radiation). An off-axis pointing requirement meant that the diagnostic had to be capable of viewing an object within 5 cm from target chamber center (TCC). However, for the early version, NIF reduced this requirement to 1 cm.

To these were added our own design requirements, such as the need to guarantee surface figure on the mirrors so that the cumulative wavefront error was within acceptable limits, to have tip/tilt adjustments on every mirror, and to have a 4-axis adjustment (translation and tip/tilt) on one large lens (L3). The lens assembly designs needed to include alignment features to assist during fielding. Integrating the VISAR diagnostic into the NIF presented a unique set of problems, such as:

- Determining that the VISAR diagnostic would be clear of interference from other beamlines (this required searching a huge CAD database)
- Assuring that the VISAR would work with the existing NIF DIM
- Addressing usability issues to insure that key system elements, operating in an aggressive environment, could be quickly accessed and repaired, if necessary. Although this especially applied to the blast window, which was most obviously susceptible to damage during an experiment, it also applied generally to all NIF equipment.
- Assuring that VISAR performance, including all actuators in the DIM, DIM cart, and steering mirrors, would be remotely monitored and controlled.

The final polar design featured a 48-m-long optical relay, 120 optical surfaces, and 65 automated adjustments. This design is slated for future installation. The shorter equatorial design had a 21-m optical path and contained 75 optical surfaces and 10 automated adjustments.

3. OPTOMECHANICAL MIRROR ANALYSIS

The first iteration of the NIF VISAR, the polar design, called for seven large mirrors, the largest (M1) to be 483 mm (19 inches) in diameter. Many of these mirrors would be mounted on the concrete ceiling or walls (Figure 3). In the polar design the mounting of mirror M1 presented a special structural problem, since it was to be sited below a central hole in the NIF target building, the “rotunda.” The installed equatorial version of the NIF VISAR has only two large,

floor-mounted mirrors (M1 and M2), the largest (M1) having a 381-mm (15-in) diameter and a 76.2-mm thickness. We suppressed stray light from the drive lasers by allowing transmission of the 1053-, 527-, and 351-nm light through the mirrors. This required supporting the mirrors on the edge with a clear aperture on the backside.

The M1 is large because of both the low f-number of the optical system and the off-axis pointing requirement. Although we initially thought the M1 mirror could move with the DIM, this proved impractical. Therefore, M1 had to contain a large enough aperture for the off-axis images.

The optical peak-to-valley (P–V) surface figure error budget for M1 was λ/4. This error budget was divided equally between manufacturing (λ/6) and mechanical deflection (λ/6), under gravity, using the root-sum-square (RSS) method:

$$\lambda/4 \approx \sqrt{(\lambda/6)^2 + (\lambda/6)^2}\,. \tag{1}$$

The surface figure requirement, diameter, and glass type determine the mirror thickness. To understand the mechanical behavior of the mirrors, consider the maximum deflection for a gravity-loaded plate (gravity vector perpendicular to the optical face) with simple[9] and 3-point[10] supporting conditions:

$$w_{max} = \frac{(5+\nu)qr^4}{64(1+\nu)D} \tag{2}$$

$$= 0.022\ Pr^2/D \text{ (simple support)}$$
$$w_{max} = 0.0362\ Pr^2/D \text{ (3-point support).}$$

$$\text{Where } D = \frac{Et^2}{12(1-\nu^2)} = \text{flexural rigidity, and} \tag{3}$$

P = total load in lbs (perpendicular to the mirror surface)
q = pressure load
E = modulus of elasticity
ν = Poisson ratio (between 0.16 and 0.24 for mirror substrates)
r = radius
t = thickness
w_{max} = maximum deflection.

Therefore, a mirror with an O-ring face support would have a much lower deflection than one with a 3-point support, but because it would have no pointing accuracy, this solution was never used. Note that the simple support condition is a good approximation of the O-ring face support. In our situation, where the gravity vector was at an angle to the mirror surface, we had to make provisions to absorb the thrust load from forces parallel to the optical surface. The mirror deflection would become much worse than the analytical solution if the 3-point contact absorbed the thrust load with friction coupling, since the 3-point contact is mounted on the surface, whereas the center of gravity is at the neutral (midplane) axis. This differential creates an unwanted moment load. The optimal place for supports is along the neutral axis; hence, the design needed to include a mounting system that behaved as though it supported the mirror there. To achieve this, we reduced friction along the 3-point contact and adding a support along the neutral axis to take up the in-plane forces.

It was thought that an O-ring support along the neutral axis would provide better support for the in-plane forces (i.e., forces parallel to the mirror surface), resulting in a simpler, more elegant design. However, because of mirrors' heavy weight, this idea proved untenable. The O-ring concept required that the mirror have a less than 1.5-mm diametrical clearance to the aluminum bore, making it difficult to install the mirrors without cocking and chipping the glass. Adding the thrust pads makes the design more complicated, but the additional diametral clearance around the mirror (except where the pad touches the glass) eases their installation and mitigates some risk.

The key metric to consider when evaluating the mirror support is the P–V deflection over the elliptical beam print (Figure 6), with any solid-body translation or rotation removed. If the three supports are clocked correctly, the P–V deflection over the beam print is about half the deflection over the full, clear aperture, because a significant percentage of the overall deflection is localized near the support (Figure 7).

We used a small amount of Permacell P440 glass tape to cover the three edge supports on M1 and M2. The tape reduced friction between the mirror and the supports so that the support behaved in the predicted fashion and mitigated any unwanted stress concentrations due to imperceptible manufacturing flaws.

With these insights, we used the parametric features of the ANSYS FEA package to develop a semiautomated procedure to analyze the mirrors' mechanical deflection. The analysis was used to establish the allowable thickness and mirror weight, which became the input parameters for the mirror support design. Note that the analytical solutions employed a thin shell approximation and thus did not exactly agree with FEA results.

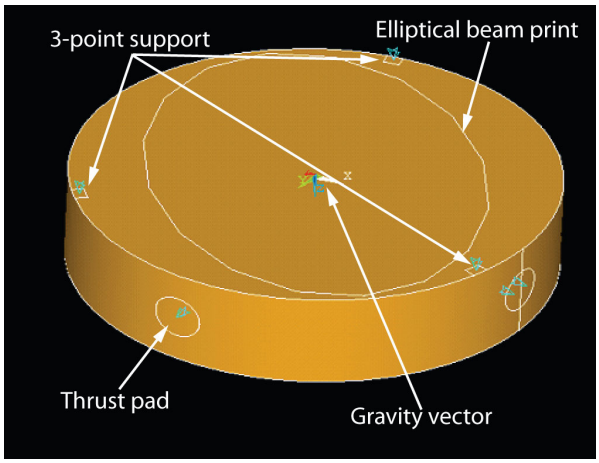

Figure 6. Mirror model

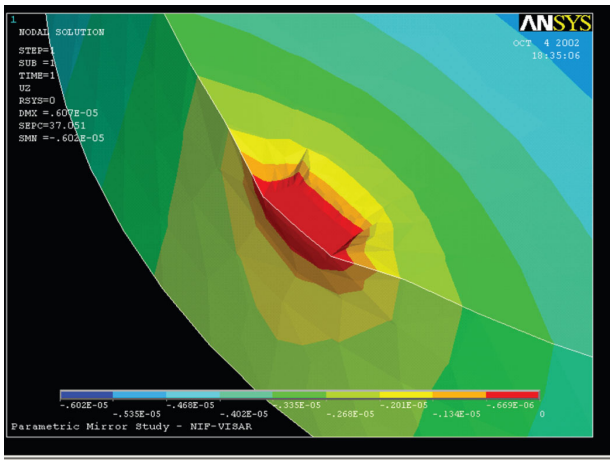

Figure 7. Local deformation of mirror support

4. MIRROR MOUNTS ANALYSIS AND DESIGN

The design of the mirror mounts addressed the following needs: (1) tip/tilt capability with axes located near the center of the optical surface, (2) a "reasonable" resonant frequency[11] (above 60 Hz if possible), (3) pointing accuracy sufficient to meet the 50-μm target specification under typical NIF vibration conditions, (4) thermal stability to meet the 4-hour alignment specification, (5) earthquake tolerance, (6) allowing unwanted drive laser light to pass through the back side of the mirror.

When thinking about the line-of-sight (LOS) requirement, it is tempting to consider an optical lever arm of the mirror that is the distance between the mirror and the target. During certain alignment steps, this will actually be the case, since the LOS is established without the optics. The lens cells are then introduced one at a time.[6] After the optics are instituted, the LOS perturbation at the target by an intermediate mirror can be shown as:

$$\delta = 2\, M\, d\, \beta, \tag{4}$$

where:

δ is a linear perturbation of the LOS at the object plane,
β is an angular perturbation of the mirror from nominal,
d is the distance from the mirror in question to the nearest intermediate image plane, and
M is the magnification between the object and nearest image plane.

The true optical lever arm of the mirror to the target is considerably less than the overall optical path length (Figures 4 and 8) when the optical elements are present. However, a mirror perturbation will cause the LOS to diverge from its intended path, creating aberrations even if the boresite errors are small.

Kinematic-style tip/tilt mounts are held together with springs, making them unattractive for very expensive mirrors. A gimbal-type design is typical for mirrors larger than 6 inches in diameter because it is "safer" than a kinematic-type design. Because of the high angular accuracy required, a flexure-type bearing was warranted. In addition, NIF specifications demanded an earthquake-tolerant design. As with previous designs[11] at NIF, this one has restraints to limit the swinging gimbal motion in the event of an earthquake (Figure 9).

Several design features increase pointing stability. The actuator mounting blocks are constructed from the same material as the actuator lead screws, thus making the design passively athermal. The actuator lead screws are coated with a solid lubricant (tungsten disulfide) to avoid dimensional instability associated with changes in oil film thickness. In general, it is better to avoid any petroleum lubricants at NIF, as they tend to contaminate the optical systems.

Results for a dynamic simulation of the M1 gimbal are presented in Figure 10. A power spectral density (PSD) graph was obtained from Lawrence Livermore National Laboratory (LLNL) to be used in the simulation. The finite element model of the gimbals was modeled using beam elements for the rings and shell elements for the mirror and outer housing. These components were connected using rigid beam elements with the appropriate degrees of freedom released to approximate the flexibility of the flex-pivots. The actuator connection was approximated by an extra boundary condition. The glass was connected to the inner ring with three beams that were oriented correctly with respect to the pivot points. ANSYS was controlled by a batch file that was fully parameterized, so that other gimbal configurations could be quickly tested. The structural assumptions were very conservative: 1% damping, the input power spectral density enveloped the LLNL graph.

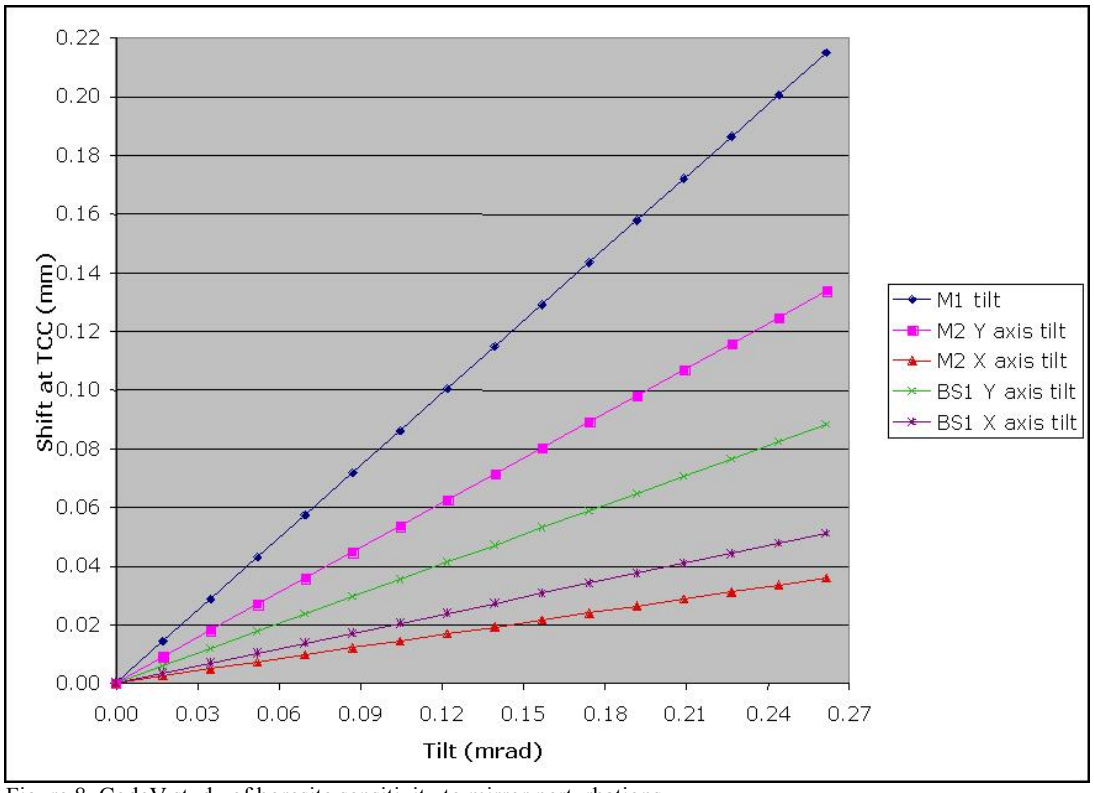

Figure 8. CodeV study of boresite sensitivity to mirror perturbations

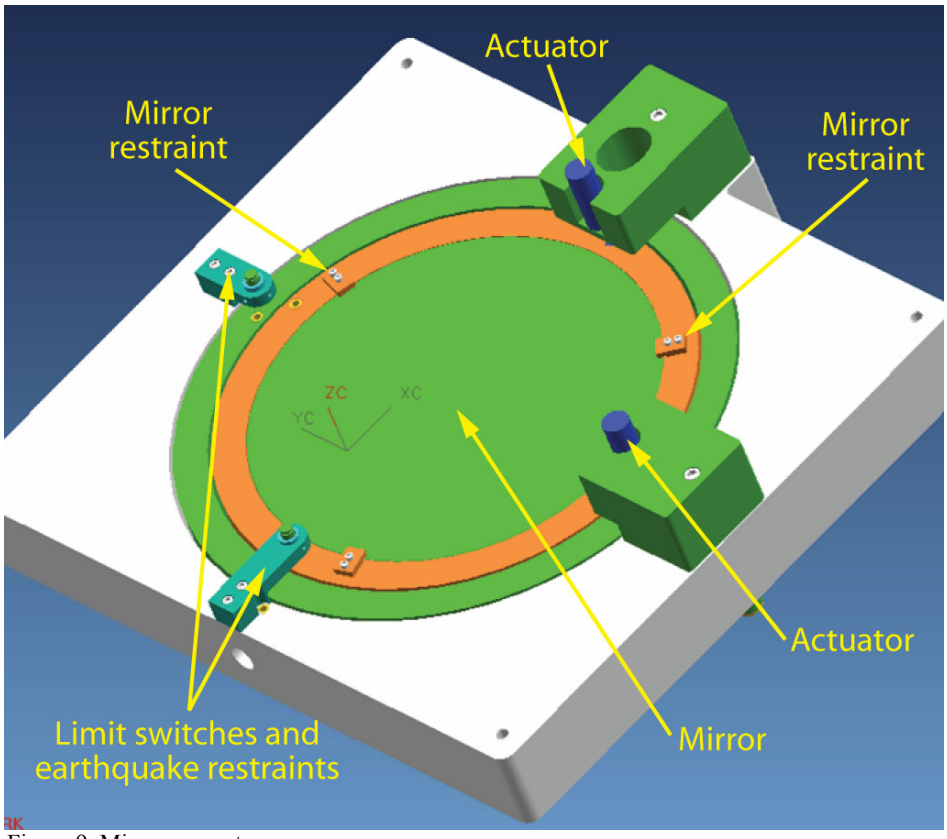

Figure 9. Mirror supports

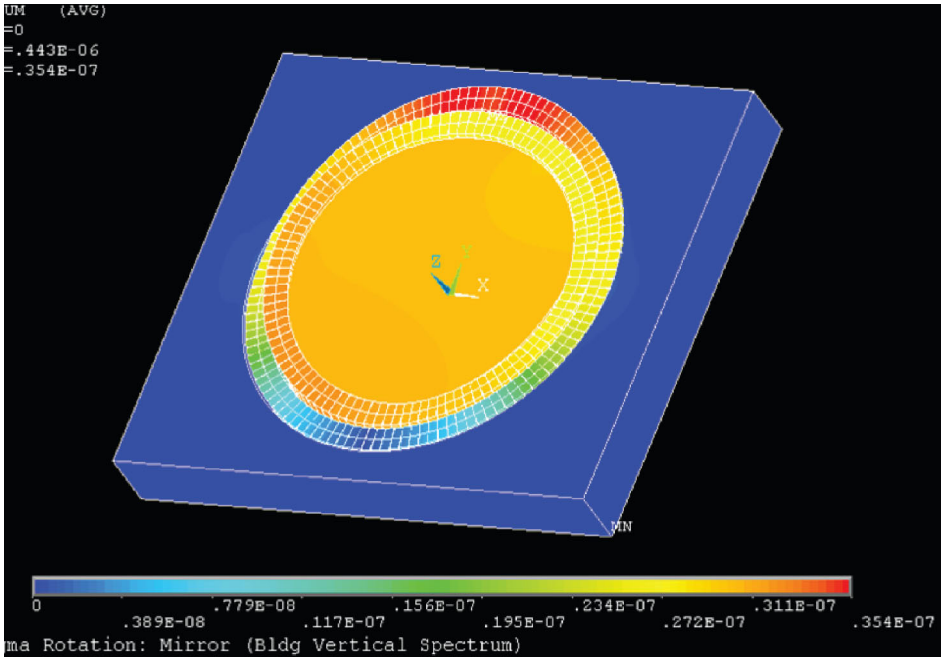

Figure 10. Vibration study of mirrors

A ray trace showed that M1 must move less than 25 μrad and M2 must move less than 50 μrad in order for the optics to meet the pointing specification of 0.025 mm at the TCC. Although it is farther from the TCC, M2 is closer to an image plane and is therefore less sensitive than M1. Assuming that the requirement applies to 3-Σ motion, the 1- Σ root-mean-square (RMS) motions of M1 and M2 should be less than 8 μrad and 16 μrad, respectively. We found that the 1-Σ motions for M1 and M2 were 0.027 μrad and 0.0071 μrad, respectively. Thus, the design is highly conservative. Fortunately, the NIF is extremely quiet. The fundamental frequency in both cases was greater than 100 Hz, which was shown to be adequate in similar situations.[11,12] During fielding in 2004, no problems associated with the gimbals' pointing accuracy or stability were apparent.

5. LENS MOUNT DESIGN

The relay lens assemblies for both the polar and equatorial designs were doublets between 6 and 14 inches in diameter. These lens assemblies required remotely actuated 4-axis adjustment, earthquake-restraint fea-tures, and internal alignment features. Alignment involved flipping the lens out of, and a reticle into, the optical path. The "pancake style" (Figure 11) is compact and simplifies mounting. Design work was minimized by making common designs for the lens and mirror gimbals. Safety and especially earthquake considerations are a hallmark of all mechanisms to be installed at NIF. During an earthquake, the limit switches double as a hard stop to avoid excessive swinging.

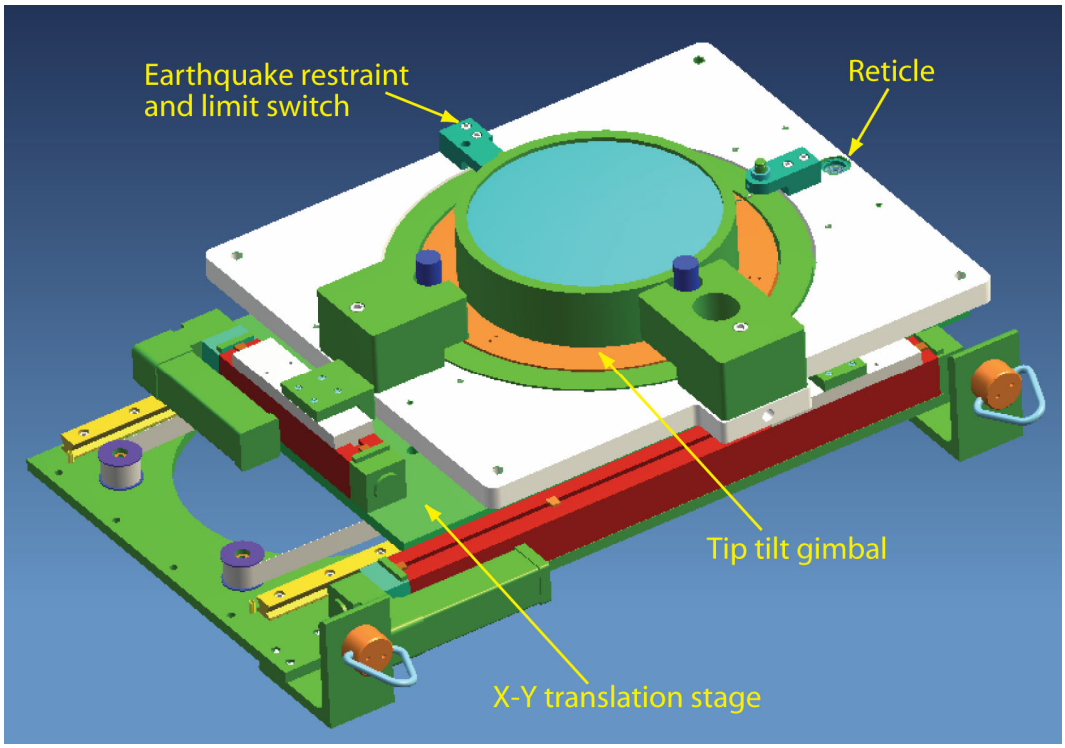

Figure 11. Four-axis automated lens supports

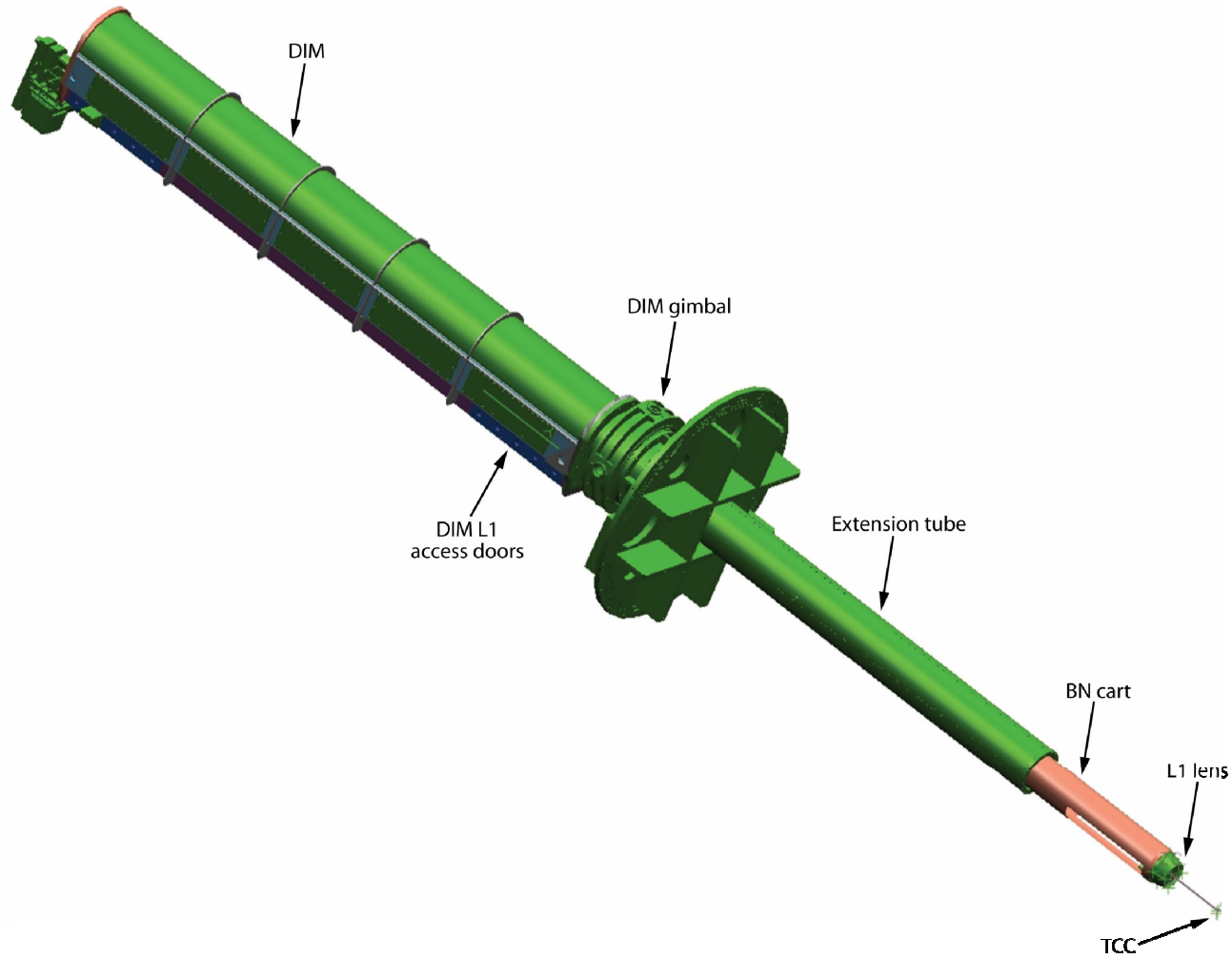

Figure 12. DIM and DIM cart in the deployed position

6. DIM CART ANALYSIS

Figure 12 shows the details of the DIM structure. Gravity-induced deflection is a factor in the equatorial configuration, due to the horizontal cantilever effect. It was necessary to account for the impact of mechanical deflection on the optical boresiting, as well as its effect on image quality due to aberrations. A very simple finite element beam and mass element model were constructed to model static and dynamic deflections from gravity and ambient vibration. At L1, a static deflection of less than 6 mm was predicted and confirmed during fielding. This deflection affected boresiting and required some of the baffles to have a slightly oblong shape. However, the deflection (both linear and angular) did not significantly affect image quality. The polar installation of VISAR will have fewer boresiting problems because of the polar DIM cart's vertical orientation.

7. CONCLUSION

The equatorial VISAR system was successfully fielded in the 90-45 equatorial port at NIF. In addition, the mission of this system has expanded to include a thermal imaging diagnostic. In the end, the optomechanical system maintained diffraction-limited performance. The future effort involves fielding the polar system which will have a much longer optical path.

The alignment features that were built into the lens mounts proved useful during the fielding effort. The number of mirrors and gimbals in early versions of the design was large, so a simple calculation method was implemented to quickly estimate the optimal design parameters.

NIF is an extremely quiet facility (with very low levels of ambient vibration), so concerns regarding the vibration stability of the VISAR optical system, with its very long optical path and gimbaled mirrors, proved to be unwarranted. There was evidence of image motion due to temperature fluctuations inside the interferometer enclosure. This problem was solved once the VISAR interferometer was reinstalled on a fully kinematic mount with a more robust lens-mounting system.[7]

NIF certainly presents an interesting challenge for the optomechanical engineer. The NIF chamber is a spacelike environment with both vacuum states and potentially high radiation levels. As NIF commissions additional drive lasers, any optical instrument will require detectors located outside the 30-m NIF target bay because of the high-radiation environment. Future VISAR work will be affected by the more stringent radiation compatibility requirements, even though VISAR will not be used for fusion experiments. To minimize the need for human interaction, any instrumentation housed within the target bay should be automated. For example, the automated alignment features in the relay lens assemblies have simplified VISAR operations. The designer must make every effort to minimize complexity and effort where human intervention is needed. Optical systems near the target chamber center require a blast shield that will need to be frequently cleaned and occasionally changed.

REFERENCES

1. L. M. Barker and R. E. Hollenbach, "Laser interferometer for measuring high velocities of any reflecting surface," *J. Appl. Phys.* **43**, 4669 (1972).
2. L. M. Barker and K. W. Schuler, "Correction to the velocity-per-fringe relationship for the VISAR interferometer," *J. Appl. Phys.* **45,** 3692 (1974).
3. D. D. Bloomquist and S. A. Sheffield, "Optically recording interferometer for velocity measurements with sub-nanosecond resolution," *J. Appl. Phys.* **54**, 1717 (1983).
4. D. H. Munro, P. M. Celliers, G. W. Collins, D. M. Gold, L. B. Da Silva, S. W. Haan, R. C. Cauble, B. A. Hammel, and W. W. Hsing, "Shock timing technique for the National Ignition Facility," *Physics of Plasmas* **8**, 2245 (2001).
5. R. M. Malone, B. C. Frogget, M. I. Kaufman, P. W. Watts, P. M. Bell, J. R. Celeste, T. L. Lee, "Design of an imaging VISAR diagnostic for the National Ignition Facility (NIF)," *SPIE Proc.* **5173**, 26–37 (2003).
6. R. M. Malone, G. A. Capelle, B. C. Frogget, R. L. Guyton, M. I. Kaufman, G. A. Lare, T. W. Tunnell, P. W. Watts, J. R. Bower, J. R. Celeste, P. M. Celliers, T. L. Lee, B. J. MacGowan, S. Montelongo, E. W. Ng, T. L. Thomas, "Fielding of an imaging VISAR diagnostic at the National Ignition Facility (NIF)," *SPIE Proc.* **5523**, 148–157 (2004).
7. R. M. Malone, J. R. Bower, D. K. Bradley, G. A. Capelle, J. R. Celeste, P. M. Celliers, G. W. Collins, M. J. Eckart, J. H. Eggert, B. C. Frogget, R. L. Guyton, D. G. Hicks, M. I. Kaufman, B. J. MacGowan, S. Montelongo, E. W. Ng, R. B. Robinson, T. W. Tunnell, P. W. Watts, P. G. Zapata, "Imaging VISAR diagnostic for the National Ignition Facility (NIF)," *SPIE Proc.* **5580**, 505–516 (2004).
8. R. M. Malone, J. R. Celeste, P. M. Celliers, B. C. Frogget, R. L. Guyton, M. I. Kaufman, T. L. Lee, B.J. MacGowan, E. W. Ng, I. P. Reinbachs, R. B. Robinson, L. G. Seppala, T. W. Tunnell, P. W. Watts, "Combining a thermal-imaging diagnostic with an existing imaging VISAR diagnostic at the National Ignition Facility (NIF)," in *Current Developments in Lens Design and Optical Engineering VI*, *Proc. SPIE* **5874**, 87–94 (2005).
9. S. Timoshenko and S. Woinowsky-Krieger, *Theory of Plates and Shells,* McGraw-Hill, New York, 1987, 57.
10. M. K. Cho, *Structural deflections and optical performance of light-weight mirrors*. PhD thesis. University of Arizona, Tucson, 1989.
11. G. L. Tietbohl, S. C. Sommer, "Stability design considerations for mirror support systems in ICF lasers," *SPIE Proc.* **3047**, 649–660 (1997).
12. G. L. Tietbohl, R. Hamilton, "Design of a Ø94 cm Mirror Mount for the Petawatt Project on Nova," Lawrence Livermore National Lab, UCRL-ID-122342 (1995).